J. Am. Chem. Soc. **1989**, *111*, 7387-7392 7387

and by substituting in terms of x, y, and c, the expression becomes:

$$x/y = cx + k_H/k_D + c \tag{16}$$

The linear relationship of the variables x/y and x in eq 16 provides a measure of k_H/k_D from the slope and intercept. Using abundance data determined under PPNICI conditions, values of $k_H/k_D = 1.2 \pm 0.1$ and 1.3 ± 0.1 were determined from eq 16 for reactions with MeO^- and e, respectively.

Calculation of Axial-Equatorial Selectivity. The source of $(M-H)^-$ ions from the reaction of **2c** with a negative ion, for example, methoxide, is through loss of the axial hydrogen at C2 (specific rate = ${}^Hk_{ax}$) and loss of hydrogen from the rear of the molecule (specific rate = k_S). The source of $(M-D)^-$ is from loss of equatorial deuterium at C2 only (specific rate = ${}^Dk_{eq}$). The respective rate expressions are:

$$d(M-D)^-/dt = {}^Dk_{eq}[\mathbf{2c}][MeO^-]$$

$$d(M-H)^-/dt = ({}^Hk_{ax} + k_S)[\mathbf{2c}][MeO^-]$$

$$\frac{d(M-D)^-/dt}{d(M-H)^-/dt} = \frac{(M-D)^-_{2c}}{(M-H)^-_{2c}} = y = \frac{{}^Dk_{eq}}{({}^Hk_{ax} + k_S)} \tag{17}$$

Dividing one expression by the other gives the relative rates in terms of relative ion abundance and specific rates (eq 17). A comparable equation relates the ion abundance data from the dideuterated compound **2b** with specific rates of hydrogen loss (eq 18). Eliminating k_S from eq

$$\frac{(M-D)^-_{2b}}{(M-H)^-_{2b}} = x = ({}^Dk_{ax} + {}^Dk_{eq})/k_S \tag{18}$$

17 and 18 and recalling that ${}^Hk_{ax}/{}^Dk_{ax} = {}^Hk_{eq}/{}^Dk_{eq} = k_H/k_D$, the following expression results:

$$k_{ax}/k_{eq} = \frac{x - y}{y(1 + [k_H/k_D]x)} \tag{14}$$

The expression for the k_{ax}/k_{eq} value for *axially* substituted **2d** was derived in a comparable manner and is given in eq 15, where y equals the abundance ratio $(M-D)^-/(M-H)^-$ from **2d** and x equals that from **2b**.

$$k_{ax}/k_{eq} = \frac{y(1 + [k_H/k_D]x)}{x - y} \tag{15}$$

Gas-Phase Base-Induced Elimination Reactions in Onium Intermediates. 1. Competitive Substitution and Elimination Mechanisms in the Attack of Amines on Diethylmethyloxonium Ions

Giorgio Occhiucci,[†] Maurizio Speranza,[*,‡] Leo J. de Koning,[§] and Nico M. M. Nibbering[§]

Contribution from the Istituto di Chimica Nucleare del CNR, 00016 Monterotondo Stazione, Rome, Italy, the Dipartimento di Agrobiologia ed Agrochimica, Università della Tuscia, 01100 Viterbo, Italy, and the Institute of Mass Spectrometry, University of Amsterdam, 1018 WS Amsterdam, The Netherlands. *Received May 17, 1988*

Abstract: The elimination/substitution branching ratio associated with the attack of amines on diethylmethyloxonium ions has been studied in the gas phase by using the method of Fourier transform ion cyclotron resonance (FT-ICR) mass spectrometry. Increasing the base strength causes enhancement of the efficiency of the elimination process relative to substitution. The same trend is observed upon increasing the excitation energy of the encounter between the oxonium ion and the base. At low encounter excitation energies, nucleophilic displacement is flanked by an entropically favored E2 elimination mechanism. At high encounter excitation energies, these reactions are superseded by alternative entropically favored processes, characterized by an initial one-electron transfer from the amine to the oxonium ion leading to a long-lived electrostatically bound adduct involving the amine radical ion and an alkyl radical loosely bound to an ether molecule. Collapse of this adduct may involve an alkyl radical-amine ion-radical recombination (an $S_{RN}1$-like mechanism) or, alternatively, a hydrogen transfer from the present neutrals to the molecular ion of the base (an E_R1 mechanism). These proposed mechanisms are unprecedented in the field of gas-phase positive ion-molecule chemistry.

Since Ingold's first introduction in 1927,[1] base-promoted olefin-forming elimination reactions (E2) have represented an inexhaustible source of mechanistic investigations by many research groups. The interest in this class of reactions derives from the widely held view that these concerted processes involve a rate-determining step proceeding via a complex transition state (I) where both C_α–X (X = leaving group) and C_β–H bonds are partially broken and the C_α=C_β and B–H (B = base) bonds are partially formed (eq 1).

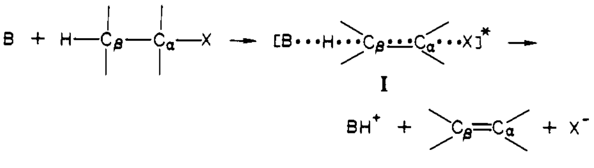

(1)

Concerted E2 mechanisms not necessarily involve synchronous cleavage and formation of bonds in I,[2] which, depending on the base strength of B, may occur via a "variable" transition state, ranging between the E1cB-like and E1-like extremes.[3] Within this concept, refinements are introduced with respect to the geometry of I involving linear C_β···H···B transfer (E2H model),[2] bent proton transfer with loose covalent interaction between nucleophilic B and C_α (E2H-E2C model),[4] and even an intermediate-type proton transfer (McLennan model).[5] In fact, the nature and the

---

[†] Istituto di Chimica Nucleare del CNR.

[‡] University of Viterbo.

[§] University of Amsterdam.

(1) (a) Hanhart, W.; Ingold, C. K. *J. Chem. Soc.* **1927**, 997. (b) Hughes, E. D.; Ingold, C. K. *Trans. Faraday Soc.* **1941**, *37*, 657.

(2) (a) Cram, D. J.; Grenn, F. D.; De Puy, C. H. *J. Am. Chem. Soc.* **1951**, *73*, 5708. (b) Bunnett, J. F. *Angew. Chem. Int. Ed. Engl.* **1962** *1*, 225. (c) *Angew. Chem.* **1962**, *74*, 731. (d) Bartsch, R. A.; Bunnett, J. F. *J. Am. Chem. Soc.* **1968**, *90*, 408.

(3) Lowry, T. H.; Richardson, K. S. *Mechanism and Theory in Organic Chemistry*; Harper and Row: New York, 1981.

(4) (a) Parker, A. J.; Ruane, M.; Biale, G.; Winstein, S. *Tetrahedron Lett.* **1968**, 2113. (b) Biale, G.; Cook, D.; Lloyd, D. J.; Parker, A. J.; Stevens, I. D. R.; Takahashi, J.; Winstein, S. *J. Am. Chem. Soc.* **1971**, *93*, 4735.

0002-7863/89/1511-7387$01.50/0

geometry of I as well as the extent of nucleophilic substitution processes, often accompanying the E2 reaction, respond to intrinsic electronic and structural requirements in the substrate and to inherent properties of the attacking base B and of the leaving moiety X. These intrinsic factors are invariably mediated in solution by specific solvation phenomena[6] so as to make reaction rates, product distribution, and even reaction stereochemistry of E2 reactions, as well as their relative extent with respect to competing substitution processes, hardly predictable.[6,7]

It has become increasingly possible to study polar E2 elimination processes in the gas phase and hence to evaluate some of the intrinsic features of the relevant transition states under conditions avoiding solvent and counterion interference. Fourier-transform ion cyclotron resonance (FT-ICR) mass spectrometry and the flowing afterglow (FA) technique have been most commonly used for this purpose, so far restricted to the study of gas-phase ionic E2 eliminations in neutral substrates induced by negatively charged bases.[8,9]

On the basis of kinetic isotope, leaving group, and conformational effect measurements, evidence was obtained with regard to the nature and the geometry (whether syn or anti periplanar) of the variable transition state involved.[9] However, apart from the reported studies of the negatively charged base-induced E2 eliminations,[8a–c,9] in general, the relative extent of the possible competing substitution pathway from the attack of the negatively charged base on the substrate cannot be determined directly as both channels give rise to the same product ion, i.e., the leaving group X$^-$.

This limitation has been avoided in the present FT-ICR study, which is aimed at investigating the mechanistic features of another class of polar E2 elimination reactions, namely those induced by neutral bases, such as amines, on positively charged oxonium ions **1** in the gas phase (eq 2). In this category of reactions, FT-ICR approach allows direct evaluation of the substitution/elimination branching ratio from the relative abundances of the ammonium ions **2–4** formed.

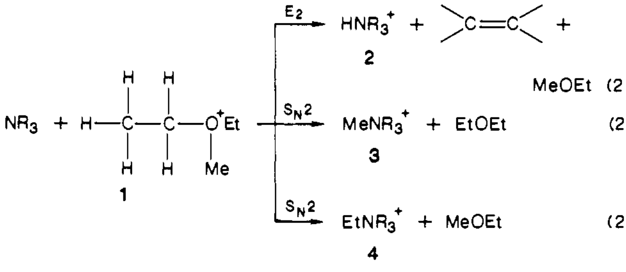

$NR_3 = NH_3$, $MeNH_2$, Me_2NH, Me_3N, $(i\text{-}Pr)_2NH$, Et_3N

In the accompanying paper, a totally different and complementary experimental approach, i.e., the radiolytic method, has been employed to investigate the stereochemistry of base-induced E2 eliminations in onium ions in the gas phase from structural analysis of the neutral products and, hence, to gain first direct information upon the syn or anti periplanar configuration of the relevant transition states.[10]

Scheme I

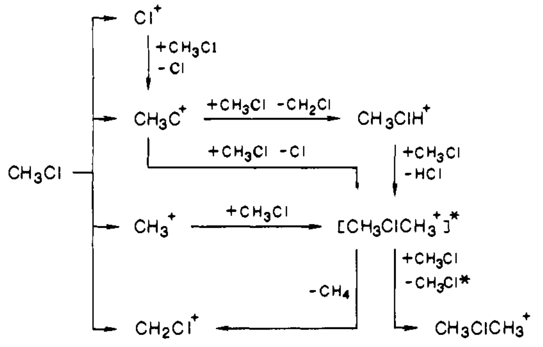

Experimental Part

Most of the experiments were performed with the homemade Fourier transform ion cyclotron resonance spectrometer of the University of Amsterdam.[11] The total pressure was always kept below 10^{-6} Torr with a background better than 2×10^{-8} Torr. Typical partial pressures used were as follows: diethyl ether, 4×10^{-7} Torr; methyl chloride, 2×10^{-7} Torr; nitrogen bases, 1×10^{-7} Torr.

Partial sample pressures were measured with an ionization gauge placed in a side arm of the main pumping line.

Positive ions were generated by 15-eV electron impact using an electron beam pulse of 20-ms duration and an emission current of 700 nA.

The ions were trapped in the magnetic field of 1.4 T by applying a small positive voltage ($\simeq$1 V) to the trapping plates of the ICR cell.

Diethylmethyloxonium ions were formed via ion–molecule reactions between $CH_3ClCH_3^+$, $CH_3Cl^{\cdot+}$, CH_3ClH^+, and diethyl ether present in the cell; the oxonium ions were isolated 500 ms after the electron beam pulse using the notch ejection technique,[12] which ejected all the ions from the cell except for the oxonium ions which were allowed to react with the neutrals present.

After a convenient reaction time ranging from 500 ms to 5 s, the cyclotroning ions were excited by a fast frequency swept radio frequency pulse with a typical sweeping rate of 1 MHz/ms and an amplitude of 10 V peak-to-peak, covering the frequency range of 1600–40 kHz and corresponding to a mass range of m/z 15–500.

The image currents, induced by translationally and coherently excited ions in the receiver plates, were monitored, digitized, and stored in a fast buffer.

After every cycle a quench pulse removed all the ions from the cell before a new cycle was started. In order to improve the signal to noise ratio, a number of cycles was accumulated, after which the digitized signal was subjected to Fourier transformation.

Peak intensities were corrected for "picket fence" errors by weighting[13] the digitized signal and for uneven excitation by trimming and deconvoluting the frequency domain signal.[14] The errors in the relative peak intensity measurements are estimated to be smaller than 5%.

Experiments involving pulsed valve addition of CH_3Cl were performed on the Bruker Spectrospin CMS 47 instrument at the University of Amsterdam. Details of this instrument and general operating procedures have been described previously.[15]

The chemicals used were commercially available. The labeled diethyl ethers were prepared by reaction of the corresponding alcohols with sulfuric acid and purified before use by preparative GC on a column of OV 17 at a temperature of 30 °C. Their label content was better than 98%.

Results and Discussion

Source of Diethylmethyloxonium Ions 1. Any comparison of gas-phase kinetic measurements with related data in solution should move from the knowledge that energy profiles of ion–molecule reactions in the diluted gas state differ from those of

---

(5) McLennan, D. J. *Tetrahedron* **1975**, *31*, 2999.

(6) (a) Cockerill, A. F. *Comprehensive Chemical Kinetics*; Elsevier: Amsterdam, The Netherlands, 1973. (b) Saunders, W. H., Jr.; Cockerill, A. F. *Mechanism of Elimination Reactions*; Wiley: New York, 1973.

(7) (a) Bartsch, R. A.; Zavada, J. *Chem. Rev.* **1980**, *80*, 454. (b) Saunders, W. H., Jr. *Acc. Chem. Res.* **1976**, *8*, 19. (c) Bartsch, R. A. *Acc. Chem. Res.* **1975**, *8*, 239. (d) Isaacs, N. S. *Annual Reports on the Progress of Chemistry*; Royal Society Chemical: London, 1970.

(8) (a) De Puy, C. H.; Bierbaum, V. M. *J. Am. Chem. Soc.* **1981**, *103*, 5034. (b) De Puy, C. H.; Beedle, E. C.; Bierbaum, V. M. *J. Am. Chem. Soc.* **1982**, *104*, 6483. (c) Bierbaum, V. M.; Filley, J.; De Puy, C. H.; Jarrold, M. F.; Bowers, M. T. *J. Am. Chem. Soc.* **1985**, *107*, 2818. (d) Sullivan, S. A.; Beauchamp, J. L. *J. Am. Chem. Soc.* **1976**, *98*, 1160. (e) Sullivan, S. A.; Beauchamp, J. L. *J. Am. Chem. Soc.* **1977**, *99*, 5017. (f) Ridge, D. P.; Beauchamp, J. L. *J. Am. Chem. Soc.* **1974**, *96*, 637. (g) van Doorn, R.; Jennings, K. R. *Org. Mass Spectrom.* **1981**, *16*, 397.

(9) (a) de Koning, L. J.; Nibbering, N. M. M. *J. Am. Chem. Soc.* **1987**, *109*, 1715. (b) Van Berkel, W. W.; de Koning, L. J.; Nibbering, N. M. M. *J. Am. Chem. Soc.* **1987**, *109*, 7602.

(10) Angelini, G.; Lilla, G.; Speranza, M. *J. Am. Chem. Soc.*, following paper in this issue.

(11) (a) For hardware, see: Dawson, J. H. J. *Lect. Notes Chem.* **1982**, *31*, 331. (b) For software, see: Noest, A. J.; Kort, C. W. F. *Comput. Chem.* **1982**, *6*, 111.

(12) (a) Noest, A. J.; Kort, C. W. F. *Comput. Chem.* **1983**, *7*, 81. (b) Kleingeld, J. C.; Nibbering, N. M. M. *Tetrahedron* **1983**, *39*, 4193.

(13) Noest, A. J.; Kort, C. W. F. *Comput. Chem.* **1982**, *6*, 115.

(14) Marshall, A. G.; Roe, D. C. *J. Chem. Phys.* **1980**, *73*, 1581.

(15) de Koning, L. J.; Fokkens, R. H.; Pinkse, F. A.; Nibbering, N. M. M. *Int. J. Mass Spectrom. Ion Processes* **1987**, *77*, 95.

Scheme II

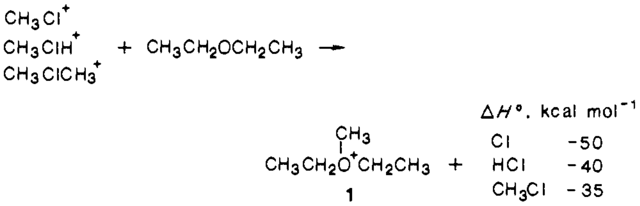

Table I. Ionic Product Distribution Resulting from the Attack of NR_3 Bases on Diethylmethyloxonium Ions **1**

base, NR_3	PA,[a] kcal mol^{-1}	product distribution: $([HNR_3^+]/([HNR_3^+] + [R'NR_3^+])) \times 100$ reaction time $t = 0.5$ s	$t = 5.0$ s
$(C_2H_5)_3N$	232.3	100[b]	100
$(iC_3H_7)_2NH$	230.2	100	100
$(CH_3)_3N$	225.1	100	80[c]
$(CH_3)_2NH$	220.6	100	60[c]
CH_3NH_2	214.1	60[c]	5[c]
NH_3	204.0	30[d]	5[d]

[a] Reference 20. [b] $NR_3^{\cdot+}$, $(NR_3{-}H)^+$, $(NR_3{-}CH_3)^+$ formed in 10%, 10%, and 15% relative yield with respect to HNR_3^+. [c] $R' = CH_3$. [d] $R' = C_2H_5$.

the same processes in the condensed phase. According to Brauman's double-well potential energy model,[16] attractive ion–neutral molecule electrostatic interaction in the gas phase results in the formation of an excited encounter complex, which is converted into a second excited complex via one or more intrinsic reaction barriers before dissociation into products. It is the shape and the relative height of these internal intrinsic energy barriers that determine kinetics and product distribution in the gas phase, which may differ from those observed in solution, where the first encounter complex is thermally equilibrated.[17] In order to approach the latter condition as much as possible and, therefore, to enable a suitable comparison of the present gas-phase FT-ICR results with those from related solution studies, the diethylmethyloxonium ion **1** (eq 2) should be prepared in the FT-ICR cell with a limited excess of internal energy. Moreover, ionic and neutral precursors of **1** should be used, which do not chemically and mass spectrometrically interfere with the reactants of eq 2 and their progeny. Satisfactory compromise was found in the dimethylchloronium ion **5**, which is able to efficiently methylate diethyl ether at the O atom producing **1**.[18]

Dimethylchloronium ion **5** is known to be readily formed, together with stable CH_2Cl^+, by the reaction pattern of Scheme I, promoted by electron impact on CH_3Cl.[19]

In fact, electron bombardment of CH_3Cl/diethyl ether gaseous mixtures generates all CH_3Cl ions of Scheme I, together with their product ions from ion–molecule reactions with diethyl ether (M), namely $[M + CH_3]^+ =$ **1** ($m/z = 89$), $[M + H]^+$ ($m/z = 75$), M^+ ($m/z = 74$), and $[M - H]^+$ ($m/z = 73$), in proportions depending upon the experimental conditions adopted. Restricting the analysis to **1** ($m/z = 89$), notch ejection[12] experiments allowed us to establish that the $CH_3ClCH_3^+$ ion is the dominant precursor of **1**, with some contributions from $CH_3Cl^{\cdot+}$ and CH_3ClH^+ (Scheme II). According to the reaction enthalpies reported in Scheme II, the procedure adopted generates oxonium ions **1** with an initial distribution of internal energy up to several tens of kilocalories per mole.

Table II. Thermochemical Data

base, NR_3	PA, kcal mol^{-1}	$\Delta H°$ reaction,[a] kcal mol^{-1} eq 2a	eq 2b	eq 2c
$(C_2H_5)_3N$	232.3	-9	-34	-34
$(iC_3H_7)_2NH$	230.2	-7	-28	-28
$(CH_3)_3N$	225.1	-1	-26	-26
$(CH_3)_2NH$	220.6	+2	-23	-23
CH_3NH_2	214.1	+9	-17	-17
NH_3	204.0	+20	-5	-6

[a] Calculated from data taken from ref 20.

Reaction of 1 with Nitrogen Bases. Reaction of **1** with NR_3 amines of different basicity, such as NH_3, CH_3NH_2, $(CH_3)_2NH$, $(CH_3)_3N$, $(iC_3H_7)_2NH$, and $(C_2H_5)_3N$,[20] results invariably in the formation of the corresponding conjugate acids HNR_3^+, accompanied by variable quantities of the alkylated fragments $R'NR_3^+$ (Table I). The ionic product distribution and the nature of the $R'NR_3^+$ fragment depend not only on the nature of the base NR_3 but also on the time lapse t between the isolation of $m/z = 89$ ion **1** and the detection of its product ions. In fact, interaction of **1** with either $(C_2H_5)_3N$ or $(iC_3H_7)_2NH$ produces exclusively the HNR_3^+ acid **2** under all conditions applied. Good yields of fragment **2** are observed as well from attack of $(CH_3)_3N$, $(CH_3)_2NH$, and CH_3NH_2 on **1**, together with $CH_3NR_3^+$ **3** in relative yields increasing with the reaction time t. A similar pattern is observed with NH_3. Here, however, $R'NR_3^+$ is not $CH_3NH_3^+$ **3** but rather the $C_2H_5NH_3^+$ ion **4**. Incidentally, it should be noted that, for $NR_3 = (C_2H_5)_3N$, at short reaction times ($t = 0.5$ s), the HNR_3^+ product is accompanied by several other ions, including $NR_3^{\cdot+}$, $[NR_3{-}H]^+$, and $[NR_3{-}CH_3]^+$ (Table I).

Formation of HNR_3^+ and $R'NR_3^+$. In principle, several mechanisms may account for the formation of HNR_3^+ and $R'NR_3^+$ in our gaseous mixtures. Apart from the classical elimination process shown in eq 2a, the HNR_3^+ fragments may arise as well from unimolecular fragmentation of the nucleophilic displacement products $C_2H_5NR_3^+$, excited by the exothermicity of their formation processes (eq 2c; Table II), with loss of a C_2H_4 moiety, as visualized in eq 3a. This possibility, can be safely ruled out by the results obtained with $NR_3 = (iC_3H_7)_2NH$. In this case, in fact, excited $C_2H_5NR_3^+$ should fragment by eliminating preferentially a C_3H_6 moiety rather than the C_2H_4 one on account of the better leaving ability of a iC_3H_7 group.[21] Consequently, a $(iC_3H_7)(C_2H_5)NH_2^+$ fragment is expected to be observed, in contrast with the experimental results. In addition, any conceivable excited $(C_2H_5)_3NC_2D_5^+$ intermediate produced via nucleophilic displacement on $(CD_3CD_2)_2OCH_3^+$ (**1b**) by $(C_2H_5)_3N$ (vide infra) would fragment yielding both $(C_2H_5)_3ND^+$ and $(C_2H_5)_2(C_2D_5)NH^+$, with the latter in higher proportions. As a matter of fact, only $(C_2H_5)_3ND^+$ and not $(C_2H_5)_2(C_2D_5)NH^+$ is observed in these experiments excluding unimolecular fragmentation of excited $C_2H_5NR_3^+$ as a significant source of the HNR_3^+ products. Another source of HNR_3^+ may, in principle, be represented by the NR_3-induced elimination on the substitution intermediate $C_2H_5NR_3^+$ shown in eq 3b. However, predominant formation of $(C_2H_5)_3ND^+$ in the $(CD_3CD_2)_2OCH_3^+$ (**1b**)/$(C_2H_5)_3N$ systems rules out as well this route to HNR_3^+. In fact, attack of $(C_2H_5)_3N$ at the β hydrogens of the substitution intermediate $(C_2H_5)_3NC_2D_5^+$ would produce both $(C_2H_5)_3ND^+$ and $(C_2H_5)_3NH^+$, with the latter prevailing over the first in contrast with experimental evidence.

$$[C_2H_5NR_3^+]^* \rightarrow [\overset{\delta+}{C_2H_5}\cdots\overset{\delta+}{NR_3}]^* \rightarrow HNR_3^+ + C_2H_4 \quad (3a)$$

$$NR_3 + C_2H_5NR_3^+ \rightarrow HNR_3^+ + C_2H_4 + NR_3 \quad (3b)$$

In the formation of the $CH_3NR_3^+$ ion, a direct nucleophilic displacement reaction between NR_3 and **1** (eq 2b) may, in principle, be accompanied by a similar process, involving methyl

---

(16) Olmstead, W. N.; Brauman, J. I. *J. Am. Chem. Soc.* **1977**, *99*, 4219.

(17) Speranza, M.; Laguzzi, G. *J. Am. Chem. Soc.* **1988**, *110*, 30.

(18) (a) Sen Sharma, D. K.; Kebarle, P. *J. Am. Chem. Soc.* **1982**, *104*, 19. (b) Speranza, M.; Pepe, N.; Cipollini, R. *J. Chem. Soc., Perkin Trans. 2* **1979**, 1179. (c) Pepe, N.; Speranza, M. *Ibid.* **1981**, 1430. (d) Speranza, M.; Angelini, G. *J. Am. Chem. Soc.* **1980**, *102*, 3115. (e) Angelini, G.; Speranza, M. *Ibid.* **1981**, *103*, 3792. (f) *Ibid.* 3800. (g) Colosimo, M.; Bucci, R. *J. Phys. Chem.* **1979**, *83*, 1952.

(19) Beauchamp, J. L.; Holtz, D.; Woodgate, S. D.; Patt, S. L. *J. Am. Chem. Soc.* **1972**, *94*, 2798.

(20) Lias, S. G.; Liebman, J. F.; Levin, R. D. *J. Phys. Chem. Ref. Data* **1984**, *13*, 695.

(21) Fornarini, S.; Speranza, M. *J. Chem. Soc., Perkin Trans. 2* **1984**, 171.

Table III. Ionic Product Distribution Resulting from the Attack of NR_3 Bases on Deuterium-Labeled Diethylmethyloxonium Ions **1a,b**

base, NR_3	oxonium ion	product distribution,[a] % DNR_3^+	HNR_3^+	NR_3^+	$(NR_3\text{-}H)^+$	$(NR_3\text{-}CH_3)^+$	$[HNR_3^+]/[DNR_3^+]$ ratio
$(C_2H_5)_3N$	**1a**	38	38	7	7	10	1.0
$(iC_3H_7)_2NH$	**1a**	26	74				2.9
$(CH_3)_3N$	**1a**	25	75				3.0
$(C_2H_5)_3N$	**1b**	52	22	8	7	11	0.4
$(iC_3H_7)_2NH$	**1b**	43	57				1.3
$(CH_3)_3N$	**1b**	47	53				1.1

[a] Reaction time, t = 1.0 s.

Table IV. Translational Energy Effect on the Product Distribution Resulting from Attack of NR_3 Bases on **1a**

E_{kin} of **1a**, eV	$[HNR_3^+]/[DNR_3^+]$ ratios NR_3 = $(CH_3)_3N$	NR_3 = $(iC_3H_7)_2NH$	NR_3 = $(C_2H_5)_3N$
~0	*a*	0.67	0.36
0.3	*a*	0.77	0.40
0.6	*a*	0.71	0.43
2.5	0.00	0.91[b]	0.62[e]
5	0.12	1.00[c]	0.71[e]
10	0.30[b]	1.43[d]	0.91[f]
20			1.11[g]

[a] The $(CH_3)_4N^+$ product is exclusively formed. [b] 3% $NR_3^{•+}$ formed as well. [c] 4% $NR_3^{•+}$ formed as well. [d] 6% $NR_3^{•+}$ formed as well. [e] 2% $(NR_3\text{–}H)^+$ and 5% $(NR_3\text{–}CH_3)^+$ formed as well. [f] 3% $(NR_3\text{–}H)^+$ and 6% $(NR_3\text{–}CH_3)^+$ formed as well. [g] 4% $(NR_3\text{–}H)^+$ and 7% $(NR_3\text{–}CH_3)^+$ formed as well.

amines NR_3 and their conjugate acids HNR_3^+, yielding again the $CH_3NR_3^+$ products (eq 4).

$$Me_{3-x}NH_x + Me_{3-x}NH_{1+x}^+ \rightarrow Me_{4-x}NH_x^+ + Me_{2-x}NH_{1+x} \quad (4)$$

$$x = 0\text{–}2$$

The efficiency of these exothermic processes ($-\Delta H°$ reaction (kcal mol^{-1}) = 12 (x = 2); 6 (x = 1); 3 (x = 0))[20] has been independently investigated in CH_3Cl/NR_3 gaseous mixtures, using the same conditions employed in the runs with **1**. Low-efficiency channels 4 have been actually observed in these systems with rates strongly decreasing with decrease of exothermicity of the process ($x = 2 > x = 1 > x = 0$). It is concluded, that this methyl transfer may contribute to the formation of $CH_3NR_3^+$ in our systems to a very minor extent, if any. This conclusion is further confirmed by notch ejection experiments carried out in the relevant systems with **1** pointing to the lack of any significant precursor–product relationship between the HNR_3^+, $R'NR_3^+$, and $NR^{•+}$ species of Table I.

The above considerations indicate that HNR_3^+ and $R'NR_3^+$ ions arise essentially from independently competing reaction channels, such as visualized in eq 2, without any significant cross contribution.

Taking into account the thermochemical data of Table II, the observation of HNR_3^+ ions in the reaction with NH_3, CH_3NH_2, and $(CH_3)_2NH$ suggests that a significant fraction of the oxonium ion **1**, generated by the reactions of Scheme II, possesses an internal energy excess sufficient to overcome the corresponding reaction endothermicities. When both thermochemically allowed, the entropically favored elimination pathway 2a appears to overwhelm the competing enthalpy-favored substitution channels (Table I). It may be concluded that, at short reaction times (t = 0.5 s), the product distribution reflects the interaction of NR_3 with oxonium ions **1** with relatively high internal energy sufficient to promote the fast high-energy entropically favored elimination process 2a yielding HNR_3^+. At longer reaction times (t = 5.0 s), a different product distribution superimposes to the t = 0.5 s one reflecting the predominant production of $R'NR_3^+$ by the comparatively slow low-energy substitution channels 2b,c. These low-energy processes involve nucleophilic attack of NR_3 on the residual fraction of **1** to give encounter complexes with an internal energy below the energy barrier for the elimination path 2a but sufficient to overcome the activation energies of the competing substitution channels 2b,c.

However, the mechanisms of formation of HNR_3^+, $R'NR_3$, and $NR_3^{•+}$ and its fragments from attack of NR_3 on **1** appear not to be straightforward in most cases, as has been revealed by studying the reactions with specifically deuterated oxonium ions **1** and investigating the relevant product distributions as a function of their excess energy.

Elimination and Substitution Mechanisms. In order to elucidate the mechanism of the base-induced elimination reactions leading to HNR_3^+ (eq 2a), the attack of $(CH_3)_3N$, $(iC_3H_7)_2NH$, and $(C_2H_5)_3N$ on specifically labeled diethylmethyloxonium ions **1a** and **1b** has been investigated (eq 5 and 6). Rather unexpectedly, interaction of the selected bases with **1a** (or **1b**) yields both the DNR_3^+ and HNR_3^+ ions (Table III). A conceivable process involving primary formation of DNR_3^+ from eq 2a, followed by hydrogen/deuterium exchange by collision with the neutrals present, may account for the occurrence of the HNR_3^+ products. Notch ejection procedures on DNR_3^+, HNR_3^+, and $NR_3^{•+}$, seem to exclude significant cross contributions among these species. In order to investigate whether DNR_3^+, HNR_3^+, and $NR_3^{•+}$ are primary products from interaction of NR_3 and **1a** (or **1b**), experiments have been performed where a large quantity of $CH_3ClCH_3^+$ ions was generated by electron bombardment on CH_3Cl injected at high pressure in the cell through a pulsed valve addition. The neutral CH_3Cl was pumped away, until the normal low pressure typical of FT-ICR experiments was achieved. Then, the deuterated ether was allowed to react with $CH_3ClCH_3^+$ to give **1a** (or **1b**) in very high amounts, which were isolated and allowed to react with NR_3. In this way, interfering reactions with neutral CH_3Cl could be avoided. By working at sufficiently low partial pressures of both the ether (2.5 × 10^{-7} Torr) and, especially, NR_3 (0.7 × 10^{-7} Torr) and by observing the reaction pattern at a very short reaction time (t = 100 ms), a DNR_3^+, HNR_3^+, and $NR_3^{•+}$ distribution is observed, which parallels that measured in the normal FT-ICR runs, thus confirming that these are primary product ions arising directly from interaction of **1a** (or **1b**) with NR_3.

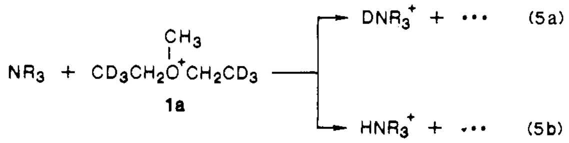

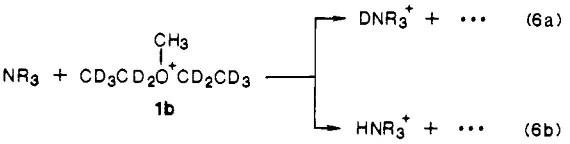

As shown in Table III, the HNR_3^+/DNR_3^+ ratios from the reactions visualized by eq 5 and 6 appear to depend upon many factors, including the nature of the base, although no simple correlations could be established between the strength of the base and the HNR_3^+/DNR_3^+ ratio. The HNR_3^+/DNR_3^+ ratio decreases by increasing the deuterium content of the diethylmethyloxonium ion (**1a** vs **1b**). The same trend is observed by increasing the reaction time t.

Table V. Translation Energy Effect on the Product Distribution Resulting from Attack of NR_3 Bases on **1b**

E_{kin} of **1b**, eV	$[HNR_3^+]/[DNR_3^+]$ ratios		
	$NR_3 = (CH_3)_3N$	$NR_3 = (iC_3H_7)_2NH$	$NR_3 = (C_2H_5)_3N$
~0	*a*	0.14	0.00
1.2	*a*	0.20[d]	0.12[f]
2.5	*a*	0.28[d]	0.17[f]
5	0.00	0.37[e]	0.27[f]
10	0.15[b]	0.50[e]	0.31[f]
20	0.50[c]		

[a] The $(CH_3)_4N^+$ product is exclusively formed. [b] 3% $NR_3^{\cdot+}$ formed as well. [c] 5% $NR_3^{\cdot+}$ formed as well. [d] 3% $NR_3^{\cdot+}$ formed as well. [e] 4% $NR_3^{\cdot+}$ formed as well. [f] $(NR_3-H)^+$ ion ($m/z = 100$) interferes with natural ^{13}C isotope containing **1b**; $(NR_3-CH_3)^+$ ion ($m/z = 86$) interferes with $(CD_3CD_2)_2OD^+$.

In view of the expected influence of the excess energy of **1a** (or **1b**) upon the course of their reaction channels, the effect was investigated of variation of the energy of the reactants on the HNR_3^+/DNR_3^+ ratio and on the abundance of $NR_3^{\cdot+}$ and its fragments. For this purpose, the excited diethylmethyloxonium ions **1a** and **1b**, generated as in Scheme II, were isolated from the corresponding reaction mixtures by means of a notch ejection pulse and allowed to collisionally quench for 1 s with the present neutrals. The nonreactive collisions yielded ground-state **1a** (and **1b**) ion, which was isolated again and, subsequently, translationally excited by applying a pulse with the cyclotron resonance frequency of **1a** (or **1b**) to the transmitter plates of the FT-ICR cell, after which **1a** (or **1b**) was allowed to react with $NR_3 = (CH_3)_3N$, $(iC_3H_7)_2NH$, and $(C_2H_5)_3N$, for $t = 2.0$ s. By varying the energy level of the radio frequency pulse, the apparent HNR_3^+/DNR_3^+ ratio has been measured as a function of the translational energy E_{kin} of **1a** (or **1b**) with E_{kin} calculated from eq 7,[22] where q is the

$$E_{kin} = \frac{q^2 V_{rf}^2 t_i^2}{8md^2} \qquad (7)$$

ion charge, V_{rf} is the energy level of the radio frequency pulse in volts peak-to-peak, t_i is the irradiation time, m is the ion mass, and d is the distance between the transmitter plates (Tables IV (**1a**) and V (**1b**)).

The data in Tables IV and V show that the excitation energy acquired by the electrostatically bound adducts between thermal **1a** (Table IV) or **1b** (Table V) ($E_{kin} = 0$ eV) and $(iC_3H_7)_2NH$ or $(C_2H_5)_3N$ is sufficient to overcome the intrinsic energy barriers for the formation of DNR_3^+ and HNR_3^+, although with largely different efficiency. In the case of $(CH_3)_3N$, instead, the internal barriers leading to DNR_3^+ and HNR_3^+ exceed the excitation energy of the corresponding electrostatic encounter, so that only the competitive substitution channel with lower activation energy is accessible to the reactants. As the translational energy E_{kin} of **1a** (Table IV) or **1b** (Table V) increases, the activation barrier of the elimination pathway is more and more accessible to the corresponding excited complex with $(CH_3)_3N$ to the point that the entropically favored elimination reaction overwhelms the competing substitution process. Besides, increasing the excitation level of the complex enhances the efficiency of the processes leading to both HNR_3^+ and $NR_3^{\cdot+}$ and its fragments.

In all systems investigated, at least two independent elimination mechanisms seem operative. At low encounter excitation energies, an E2 elimination reaction takes place favoring formation of DNR_3^+ over HNR_3^+. At higher encounter excitation levels, the E2 process is accompanied by an additional elimination mechanism, with a comparatively high activation energy, leading to the formation of HNR_3^+ and, possibly, $NR_3^{\cdot+}$ and its fragments. Unpredictable primary and secondary H/D isotope effects do not allow us to quantitatively estimate the relative activation barriers of the two different elimination pathways.

The data in Tables IV and V suggest that the formations of HNR_3^+ and $NR_3^{\cdot+}$ are coupled, which is indicative for a common intermediate. Most likely,[23] this intermediate is formed following an electron transfer from the amine to the oxonium ion, resulting in either one of the adducts **6** or **7**.[24] These intermediate adducts now can dissociate to give $NR_3^{\cdot+}$ or may react further to give products, as shown in eq 8.

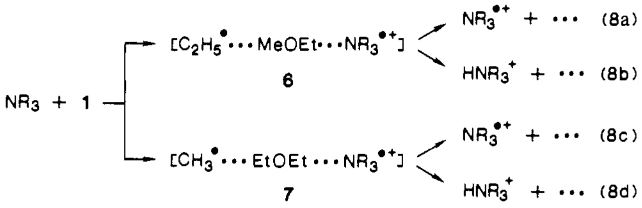

In this mechanism, overall proton transfer from **1** to the amine is initiated by electron transfer causing C–O bond elongation followed by hydrogen transfer from the alkyl moiety or the dialkyl ether to the amine radical cation. Since, in principle, all the hydrogens are abstractable, this mechanism can account for both the observations that hydrogen transfer is detected in the reaction of **1b** with amines and that deuterium transfer is enhanced relative to hydrogen transfer, when the deuterium label content of the oxonium ion **1** is increased (cf. Tables IV and V).

Statistical hydrogen transfer in the intermediate complex would result in a $[HNR_3^+]/[DNR_3^+]$ ratio of 1.17 and 0.3 for the reaction with **1a** and **1b**, respectively, values which are very close to the experimental results obtained for the reaction of translationally highly excited oxonium ions **1a** (Table IV) and **1b** (Table V). These findings strongly support the proposed reaction sequences given in eq 8, concerning the high-energy processes.

Note that, when hydrogen transfer from the alkyl radical to $NR_3^{\cdot+}$ is energetically unfavored,[25] as in the adduct **7** of eq 8c,d, recombination of $NR_3^{\cdot+}$ with the alkyl radical moiety may take place, forming the corresponding alkylammonium ion via an overall process similar to the $S_{RN}1$ mechanism, well-known in the condensed phase.[26] This implies that, for the systems studied, both the E2 and S_N2 reactions may be accompanied by alternative elimination and substitution mechanisms.

The course of the reaction appears connected not only with the overall reaction enthalpies and the excess energy deposited in the encounter complex but also with the energy gap between the LUMO orbitals of the oxonium ion and the HOMO orbitals of the amine bases. In fact, assuming that the initial electron transfer of eq 8 is most favored when it is quasi-resonant, interaction between the HOMO of $(C_2H_5)_3N$ (−8.1 eV)[27] and $(iC_3H_7)_2NH$ (−8.3 eV) and the second LUMO of **1** ($\sigma^*_{O-Et} = -7.9$ eV)[28] should

---

[22] Kleingeld, J. C. Thesis, University of Amsterdam, The Netherlands, 1984.

[23] Several alternative plausible mechanisms can be put forward to account for the data of Tables IV and V, including a concerted ylid mechanism[6] involving preliminary interaction between the base and the positively charged C_α–H proton of **1**, followed by a concerted C_α-to-NR_3 proton transfer assisted by a C_β-to-C proton shift. A similar mechanism is involved in the gas-phase elimination of thioethers induced by R_2N^- ions.[9b] The ylid mechanism, however, does not provide any simple answer to the problem of the formation of $NR_3^{\cdot+}$ and its fragments, which accompanies that of HNR_3^+. Moreover, the transition state of the ylid mechanism should be much less entropically favored with respect to the one (I) involved in the classical E2 mechanism 1, yielding exclusively DNR_3^+. As a consequence, concomitant occurrence of a high-energy ylid mechanism and of a low-energy E2 process 1 would lead to a NHR_3/DNR_3^+ product mixture, but with the HNR_3^+/DNR_3^+ yield ratio decreasing by increasing the energy level of the NR_3/**1a,b** encounter, in contrast to the experimental evidence (Tables IV and V).

[24] The processes shown in eq 8 are reminiscent of Perrin's mechanism of aromatic nitration in solution, involving preliminary electron transfer between NO_2^+ and the aromatic substrate before addition; cf.: Perrin, C. *J. Am. Chem. Soc.* **1977**, *99*, 5516. The same mechanism has been observed in the gas phase as well; cf.: Ausloos, P.; Lias, S. G. *Int. J. Chem. Kinet.* **1978**, *10*, 657.

[25] Thermochemical calculations indicate that hydrogen transfer from the methyl moiety of **7** to $NR_3^{\cdot+}$ to yield $(C_2H_5)_2O$, CH_2, and HNR_3^+ is endothermic by 37 ($(C_2H_5)_3N$), 39 ($(iC_3H_7)_2NH$), and 45 ($(CH_3)_3N$) kcal/mol.

[26] Bunnett, J. F. *Acc. Chem. Res.* **1978**, *11*, 413.

[27] The vertical ionization potential of the amine is taken as an estimate of its HOMO orbital: Aue, D. H.; Webb, H. M.; Bowers, M. T. *J. Am. Chem. Soc.* **1972**, *94*, 4728.

take place predominantly, yielding preferentially complex **6**. On the contrary, formation of complex **7** should be favored, owing to the preferred interaction of the HOMO of $(CH_3)_2NH$ (−8.8 eV) and CH_3NH_2 (−9.5 eV),[27] with the first LUMO orbital of **1** ($\sigma^*_{O-Me} = -8.6$ eV).[28] As observed, $(CH_3)_3N$ is expected to give both **6** and **7**, on account of its HOMO orbital (−8.4 eV), which is intermediate between the first and the second LUMO orbitals of **1**.

In this view, sequences 8 are presumably precluded to NH_3, owing to the much larger energy gaps between the first and second LUMO orbitals of **1** and the HOMO orbital of NH_3 (−10.9 eV).[27] As a consequence, NH_3 can only produce **4** from **1** via a classical S_N2 reaction, involving a transition state characterized by a pronounced development of the positive charge on the carbon center, in analogy with related S_N2 processes in the gas phase.[29]

In conclusion, the observed relative extent of the elimination vs substitution pathways and the nature of the substitution products **3** may be accounted for by the relative efficiency of the formation of complexes **6** and **7**, representing different electron-transfer channels.

Conclusions

The results of the present study have allowed us to directly establish the branching ratio between the overall elimination and substitution channels induced by attack of amines on specifically selected oxonium ions. In general, increasing the base strength enhances the efficiency of the E2 elimination process with respect to the S_N2 substitution one.

However, E2 and S_N2 reactions, prevailing in the interaction between the amines and thermal oxonium ions, are superseded by alternative high-energy favored mechanisms, when the oxonium ions are vibrationally or translationally excited. These processes are characterized by an initial one-electron transfer from the base to the oxonium ion, generating an electrostatically bound adduct between the molecular ion of the amine and an alkyl radical loosely bound to an ether moiety. The subsequent fate of these adducts depends on many factors, including their excitation energy and the nature of the alkyl radical and the amine radical ion. Thus, at high excitation levels, unimolecular fragmentation of the adducts takes place with formation of the amine radical ion and its fragments. At lower energies, this process is accompanied by hydrogen transfer between the alkyl radical, or the ether moiety, to the amine radical ion, yielding protonated amine. Alternatively, the amine radical ion may combine with the alkyl radical, giving rise to an alkylammonium ion. In the first case, we are facing a totally new elimination mechanism entropically favored at high energies, which can be denoted as a E_R1 process, where loss of the leaving ether group is induced by electron transfer from the base to the oxonium ion. In the second case, the alkylation resembles the well-known Bunnett's $S_{RN}1$ process, frequently involved in negative ion-induced nucleophilic aromatic displacements in solution.[26] At any rate, the present results indicate that both E_R1 and $S_{RN}1$ mechanisms take place within an intimate long-lived electrostatically bound complex, involving a radical ion and a radical loosely bound to a neutral molecule, whose occurrence, to our knowledge, was never claimed before in gas-phase positive-ion chemistry studies.[30]

A drawback of this FT-ICR study is that all the processes detected in the present systems interfere with the E2 reaction. It follows that investigation of the nature and the geometry of the relevant transition state is hardly allowed by the FT-ICR technique. A further difficulty is that the relative extent of these interfering processes is dependent on the rather unpredictable energy content of the electrostatically bound encounters between **1** and the amine. These difficulties may be removed, by resorting to a totally different technique, i.e. the high-pressure radiolytic technique, allowing thermal equilibration of the ion–molecule encounter complexes and direct analysis of the isomeric distribution of the final elimination products. An example of application of this technique to the study of gas-phase base-induced elimination on onium ions is given in the following paper.[10]

Acknowledgment. We thank F. A. Pinkse for his expert technical assistance and the Netherlands Organization for Scientific Research (SON/ZWO) for invaluable and continuous support. The financial support of the Ministero della Pubblica Istruzione and Strategic Project "Molecular Dynamics and Catalysis" of the Consiglio Nazionale delle Ricerche is also gratefully acknowledged.

---

(28) The energy levels of the first and second LUMO orbitals of **1** have been estimated as −8.6 and −7.9 eV, respectively, by LCBO calculations, using a typical 1-eV value for the β resonance parameter and the ionization potentials of Et_2O, MeOEt, $CH_3^\bullet$, and $C_2H_5^\bullet$ (Vedeneyev, V. I.; Gurvich, L. V.; Kondrat'yev, V. N.; Medvedev, V. A.; Frankevich, Ye. L. In *Bond Energies, Ionization Potentials and Electron Affinities*; Arnold, Ed.; London 1966), as a measure of the H_{ii} and H_{jj} coulombic parameters, representing the energy of the relevant unperturbed orbitals.

(29) (a) Fornarini, S.; Sparapani, C.; Speranza, M. *J. Am. Chem. Soc.* **1988**, *110*, 34. (b) Crotti, P.; Macchia, F.; Pizzabiocca, A.; Renzi, G.; Speranza, M. *Gazz. Chim. Ital.* **1987**, *117*, 739. (c) Crotti, P.; Macchia, F.; Pizzabiocca, A.; Renzi, G.; Speranza, M. *Tetrahedron Lett.* **1987**, *28*, 3393.

(30) Two-body long-lived electrostatic complexes between an ion and a neutral molecule have been frequently observed in the gas phase; see, for instance: Hunter, E. P.; Lias, S. G. *J. Phys. Chem.* **1982**, *86*, 2769.